Aquatic Botany 207 (2026) 104047

Contents lists available at ScienceDirect

Aquatic Botany

journal homepage: www.elsevier.com/locate/aquabot

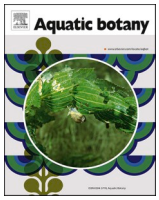

# Fruit morphology of Posidonia oceanica (L.) Delile and its relationship to floating orientation and potential surface dispersal

Trace Laskey [a,1], Arturo Zenone [b,c,d,*,2], Adriana Alagna [c,d,3], Giovanni D'Anna [d,e,4], Vincenzo Maximiliano Giacalone [d,f,5], Eduardo Infantes [g,6], Marco Martinez [h,7], Carlo Pipitone [b,d,8], Fabio Badalamenti [a,b,d,9]

[a] School of Geosciences, University of Edinburgh, The King's Buildings, Edinburgh EH9 3FE, United Kingdom
[b] Institute for the study of Anthropic impact and Sustainability in the marine environment, IAS-CNR, Palermo, Italy
[c] Sicily Marine Centre, Stazione Zoologica Anton Dohrn, Palermo, Italy
[d] National Biodiversity Future Centre (NBFC), Palermo, Italy
[e] Institute for the study of Anthropic impact and Sustainability in the marine environment, IAS-CNR, Castellammare del Golfo, Italy
[f] Institute for the study of Anthropic impact and Sustainability in the marine environment, IAS-CNR, Campobello di Mazara, Italy
[g] Department of Biology, Campus Tafira, University of Las Palmas de Gran Canaria, Las Palmas, Canary Islands 35017, Spain
[h] Institute for Environmental Protection and Research (ISPRA), Via Del Fosso Fiorano, 64, Rome 00143, Italy

ARTICLE INFO

*Keywords:*
Posidonia oceanica
Seagrass
Fruit morphology
Floating orientation
Buoyancy
Hydrochory

ABSTRACT

*Posidonia oceanica* (L.) Delile produces buoyant fruits that disperse at the sea surface, yet the morphological basis of their stable floating orientation remains poorly quantified. We combined morphometric measurements, geometric and Archimedes-based estimates, and macroscopic sectioning to test whether a recurrent dorsal protrusion, reflecting dorsoventral asymmetry, is associated with a consistent floating orientation and to describe the internal organisation associated with this dorsoventral asymmetry. Fruits showed a strong tendency to self-orient with the dorsal protrusion facing upward and maintained an emerged fraction of ~18–20% of total fruit volume under static conditions. Macroscopic sections showed that this external asymmetry corresponded to a consistent internal dorsoventral organisation, including thicker dorsal mesocarp above the seed. Simple proxies based on fruit mass and axial measurements closely matched direct measurements of mass and volume, supporting their use as practical non-destructive estimators of dispersal-relevant traits. Together, these results identify morphological traits associated with stable floating orientation in *P. oceanica* fruits and provide quantitative descriptors of the floating phase that may inform future trait-based approaches to near-surface dispersal and connectivity.

## 1. Introduction

Seagrass meadows are among the most productive coastal ecosystems and provide functions that extend well beyond their footprint (Orth et al., 2006; Unsworth et al., 2019). They create structurally complex habitats, stabilise sediments, attenuate waves, and contribute substantially to coastal oxygen production and carbon storage (Waycott et al., 2009; Infantes et al., 2012; Fourqurean et al., 2012; UNEP, 2020).

* Corresponding author at: Institute for the study of Anthropic impact and Sustainability in the marine environment, IAS-CNR, Palermo, Italy.
*E-mail address:* arturo.zenone@cnr.it (A. Zenone).
[1] 0009-0001-4299-4846
[2] 0000-0001-5540-7148
[3] 0000-0003-1697-0901
[4] 0000-0002-8644-8222
[5] 0000-0002-4316-1723
[6] 0000-0002-9724-9237
[7] 0009-0000-4983-600X
[8] 0000-0002-7632-1228
[9] 0000-0002-2395-454X

https://doi.org/10.1016/j.aquabot.2026.104047
Received 20 April 2026; Received in revised form 13 July 2026; Accepted 17 July 2026
Available online 3 August 2026

Despite their ecological and socio-economic importance, seagrass landscapes are declining in many regions, and recovery after disturbance is often slow or spatially uneven (Waycott et al., 2009; Duarte et al., 2020; Saunders et al., 2024). Accordingly, the processes that govern dispersal, colonisation, and connectivity are central to understanding persistence and recovery dynamics in seagrass habitats (Orth et al., 2006; Kendrick et al., 2012; Grech et al., 2016). As marine angiosperms, seagrasses reproduce through both clonal growth and sexual reproduction. Clonal expansion can efficiently maintain and spread meadow structure at local scales but produces genetically identical shoots and may limit dispersal beyond the immediate boundary of a meadow (Rasheed, 2004; Kendrick et al., 2012). Sexual reproduction, in contrast, generates dispersal units (propagules) represented here by seeds and fruits, which can disperse away from the source meadow and introduce new genotypes, supporting connectivity, genetic diversity, and colonisation of new suitable habitats, including sites targeted by restoration (Kendrick et al., 2012; McMahon et al., 2014).Propagule dispersal in seagrasses can occur via several pathways and its potential varies strongly among taxa (Kendrick et al., 2012; McMahon et al., 2014; Mari et al., 2020). A recurrent challenge in predicting dispersal and connectivity is that near-surface transport and subsequent establishment depend not only on external forcing such as winds, waves, and currents (Infantes et al., 2011; Zenone et al., 2022), but also on species-specific traits. Buoyancy determines whether a propagule remains at the surface and for how long, whereas shape and surface exposure influence drag at the air-sea interface (McMahon et al., 2014; Ruiz-Montoya et al., 2012). In this setting, even small differences in the fraction of a propagule exposed to air can alter the balance between current-driven drift and wind-driven motion, resulting in dispersal model sensitivity to assumptions about propagule “windage”. In practical terms, windage is not a single constant but depends on how a propagule sits at the surface. If posture is unstable, surface exposure may fluctuate, increasing uncertainty in near-surface transport predictions. Conversely, a stable orientation coupled with a reproducible emerged fraction would allow windage to be parameterised more directly, reducing reliance on tuning and improving comparability across studies and systems. Trait-based approaches provide a framework for connecting measurable properties to ecological processes in seagrass systems (Moreira-Saporiti et al., 2023). Basin-scale modelling studies suggest that ocean circulation can connect distant meadows through surface fruit transport (Mari et al., 2020; Barrier et al., 2026). Mediterranean-wide simulations of *P. oceanica* fruit dispersal further show that floating duration strongly influences the spatial footprint of potential connectivity, with longer buoyancy scenarios activating broader dispersal corridors (Barrier et al., 2026). However, the parameterisation of propagule traits in such models remains simplified particularly with respect to how floating fruits interact with the air-sea interface (Mari et al., 2020; Barrier et al., 2026). In dispersal modelling, explicitly integrating trait variability such as buoyancy and surface exposure can strongly affect predicted dispersal and connectivity patterns (McMahon et al., 2014; Mari et al., 2020; Hanuise et al., 2025). This highlights a practical gap for many seagrass species, as key traits are still not measured in ways that are comparable across populations and directly usable in dispersal models.

*Posidonia oceanica* is endemic to the Mediterranean Sea and is a foundation species that forms extensive, long-lived meadows. Sexual reproduction in *P. oceanica* is episodic, but when it occurs it can be ecologically important because it helps maintain genetic diversity within meadows and long-distance connectivity among populations. This is because the fruits act as buoyant dispersal units and can disperse potentially long distances at the sea surface before releasing seeds (Balestri and Cinelli, 2003; Kendrick et al., 2012; Ruocco et al., 2025). Sexual recruitment has been described as a sequence of stages that includes a surface dispersal phase in intact fruits and a subsequent settlement phase following fruit opening (Guerrero-Meseguer et al., 2018). The study by Guerrero-Meseguer et al. (2018) highlights the functional role of fruit structure during dispersal, including the buoyant, spongy pericarp and the potential for seeds to remain physiologically active while enclosed. Many fruits also strand on beaches, which has traditionally been viewed as a loss of reproductive investment. However, recent experiments indicate that fruit encasing can protect seeds against desiccation and viability loss, and a substantial fraction of stranded fruits and seeds can be returned to the sea by wave action (Sutera et al., 2024). Together, these findings suggest that both the floating fruit phase and transitions between offshore transport, stranding, and potential return to the sea can be relevant when interpreting dispersal potential and connectivity (Jahnke et al., 2017; Pereda-Briones et al., 2018).

These studies highlight that the fruit phase is not simply a transport container but a functional stage with its own constraints and opportunities. However, from a trait and modelling perspective, key physical descriptors of this stage remain limited for *P. oceanica*, including quantitative links between fruit morphology, stable floating orientation, and predictable surface exposure. This matters because floating orientation can determine whether a consistent portion of the fruit remains above water and whether windage remains stable through time. Without such estimates, windage is often assumed or treated as a tuning parameter in dispersal models. Filling this gap would help connect recruitment-stage descriptions with mechanistic representation of near-surface dispersal. Functional analogues from other hydrochorous systems support the expectation that floating orientation can influence dispersal outcomes by affecting surface exposure and sensitivity to wind forcing. Although dispersal structures differ among taxa, the underlying physical constraints on floating transport are comparable. Mechanistic work on mangrove propagules shows that wind can substantially influence dispersal trajectories and that species-specific sensitivity depends on propagule morphology and the portion exposed at the surface (van der Stocken et al., 2013, 2019). More generally, wind has also been shown to affect dispersal speed, distance, and deposition patterns of floating seeds in slow-flowing and stagnant waters (Sarneel et al., 2014). These functional insights provide a strong motivation to quantify *P. oceanica* fruit traits that influence floating orientation and the proportion of the fruit that remains exposed at the surface.

Here we test whether a recurrent dorsal protrusion, reflecting consistent dorsoventral asymmetry, is associated with a repeatable floating orientation and a reproducible emerged fraction in *P. oceanica* fruits. Using morphometrics, flotation trials, and macroscopic sectioning, we relate external asymmetry to internal organisation. We also evaluate simple proxy approaches for estimating dispersal-relevant traits, aiming to provide practical descriptors based on accessible measurements that can be compared across studies and used in future near-surface dispersal models. Post-collection fruit dehiscence was recorded as a complementary observation relevant to the fruit phase described here.

## 2. Materials and methods

### 2.1. Sample collection and handling

Beach-cast *Posidonia oceanica* fruits were collected along the coast of Isola delle Femmine (Gulf of Carini, north-western Sicily, central Mediterranean) between 21 and 23 April 2025 (Fig. 1). This area was selected based on previous observations identifying it as a recurrent fruit accumulation hotspot influenced by prevailing currents and drift lines (Provera et al., 2024; Ruocco et al., 2025). Sampling was conducted over three consecutive mornings immediately following strong north-westerly winds (locally, the Maestrale). Collections took place at the onset of the high-tide phase, when beach-cast material was actively deposited along the shoreline. Fruits were collected manually along the tideline by sifting through beach-cast debris and were selected based on external indicators of freshness, including intact pedicels, attached dark green sepals, and turgid pericarp tissue. Only fruits showing no visible signs of dehiscence were retained.

In total, 196 fruits were collected. Of these, 100 fruits were assigned

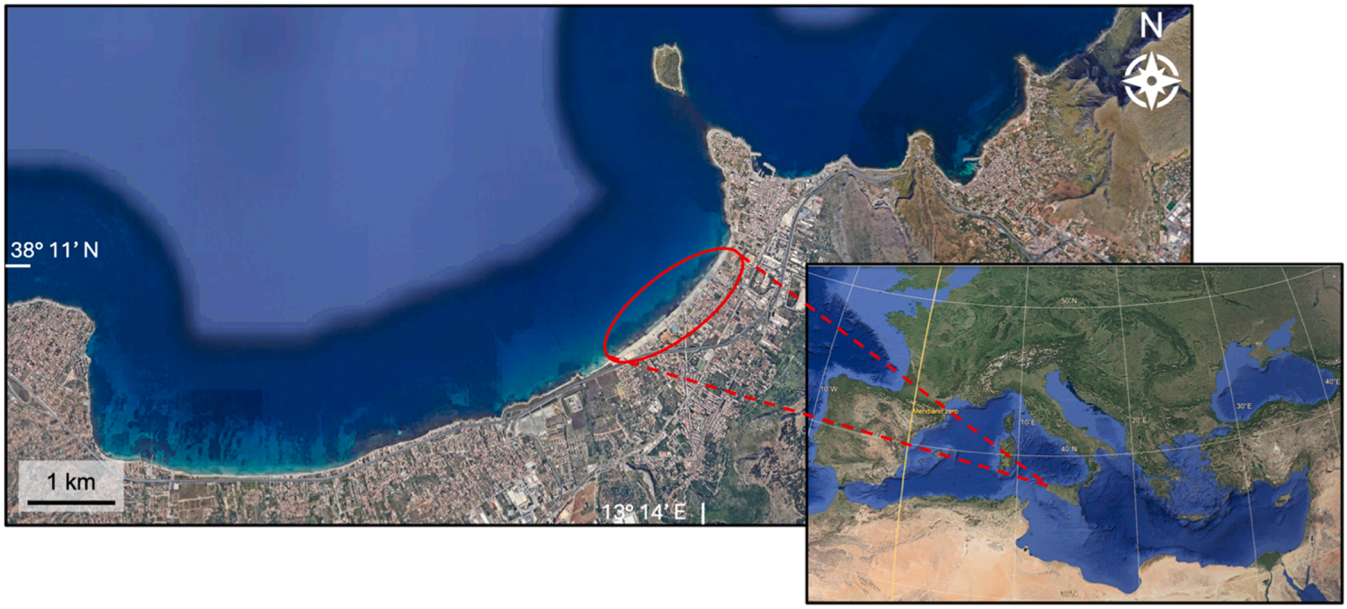


**Fig. 1.** Sampling location (red circle) along the coast of Isola delle Femmine (Gulf of Carini, NW Sicily, Italy; 38°11′ N, 13°14′ E).

to morphology-related trait analyses and 96 to dehiscence observations. Within the morphology subset, all 100 fruits were measured morphometrically, 41 were used for displacement-based volume measurements, and 18 of these 41 were further used for flotation trials and

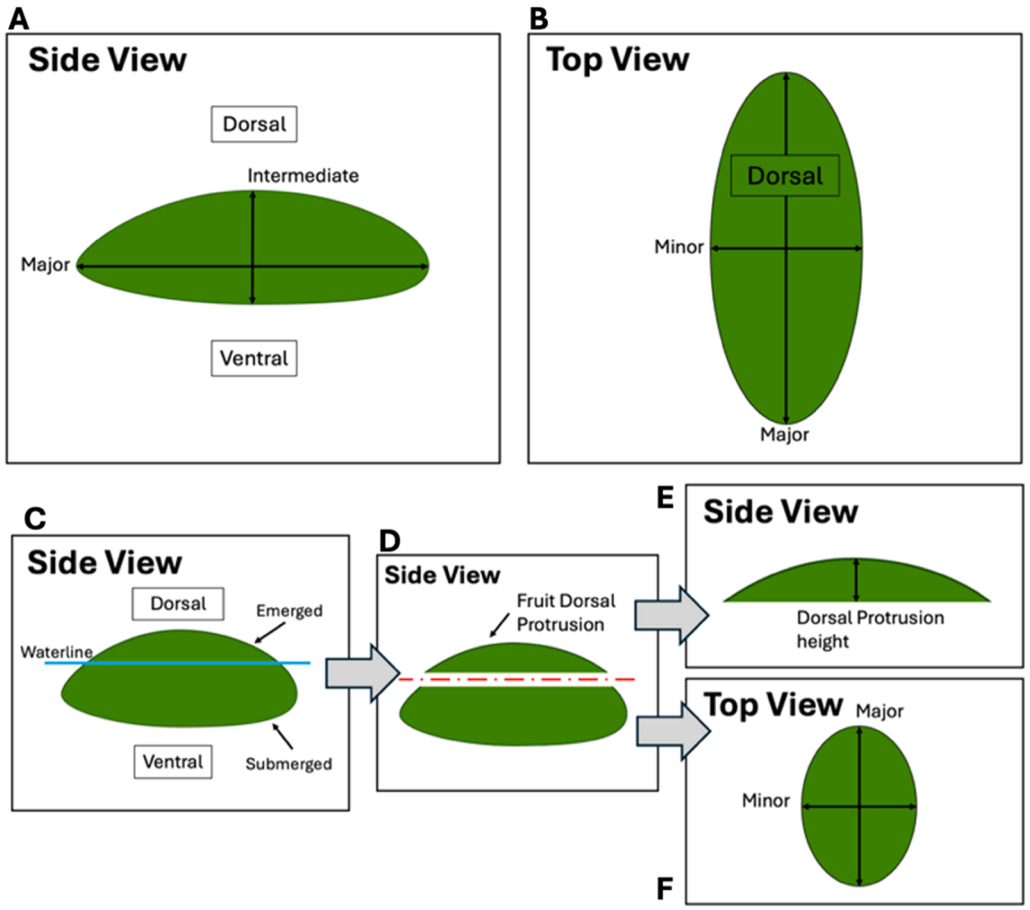


**Fig. 2.** Schematic representation of Posidonia oceanica fruit morphology, floating orientation, and dorsal protrusion measurements. **(a)** Side view of the fruit showing dorsoventral orientation and the major and intermediate axes. **(b)** Top view showing dorsoventral orientation and the major and minor axes. **(c)** Conceptual side view of a floating fruit showing the position of the waterline and the emerged and submerged portions. **(d)** Side view highlighting the emerged dorsal protrusion. **(e)** Side view illustrating the definition of dorsal protrusion height. **(f)** Top view illustrating the major and minor diameters measured at the base of the dorsal protrusion.

dorsal protrusion measurements. This progressive reduction in sample size reflects the hierarchical design of the study: while all fruits in the morphology subset were used for basic morphometric measurements, only subsets were used for displacement-based volume measurements and flotation/dorsal protrusion analyses because these procedures were more time-consuming, partly destructive, and necessary only for specific derived traits and validation steps. After collection, samples were placed in cooled seawater and transported to the laboratory, where they were stored in seawater at 4 °C and a salinity of 38‰. Salinity was maintained at values representative of local seawater, whereas refrigerated storage at 4 °C was used only to preserve fruit integrity prior to analysis and does not represent ambient field temperature. Experimental conditions for flotation and dehiscence trials are reported separately below according to the objective of each assay. Fruits used for morphological analyses were processed within 48 h of collection. Seawater was regularly renewed to maintain sample integrity. All the activities were carried out at the CNR-IAS facilities in Sicily.

### 2.2. Fruit morphology and axial measurements

Axial measurements were recorded for all 100 fruits using a digital calliper (precision 0.1 mm). The major, intermediate, and minor axes were defined as maximum fruit length, width, and thickness, respectively (Fig. 2a,b). After measurement, fruits were gently blotted with absorbent paper for approximately 10 s before wet mass (g) was determined using an analytical balance (precision ±0.0001 g). Direct wet mass measurements were used as reference values, and a multiple linear regression model was then fitted to evaluate whether fruit mass could be predicted allometrically from axial measurements as a transferable proxy when only linear dimensions are available or direct weighing is impractical, according to the following equation:

$$\text{Mass} = \beta_0 + \beta_1 a + \beta_2 b + \beta_3 c$$

where $a$, $b$, and $c$ are the major, intermediate, and minor axes, respectively.

After axial measurements, 59 of the 100 fruits were frozen for long-term storage and future analyses and were not used in subsequent displacement, excision, flotation, or orientation analyses, while the remaining 41 fruits were used to determine fruit volume by seawater displacement in a graduated cylinder (resolution 1 mL = 1 $cm^3$). A thin wooden dowel was used to fully submerge each fruit. Prior testing confirmed that inserting the dowel approximately 1 cm into the water did not alter the volume reading.

### 2.3. Fruit mass, volume, density and surface area

Fruit volume was also estimated for all 100 fruits from axial measurements by approximating each fruit as triaxial ellipsoids. This was done to evaluate whether simple linear dimensions could provide a practical geometric proxy for fruit volume across the full dataset. The model took the following form:

$$V = \frac{4}{3}\pi\left(\frac{a}{2}\right)\left(\frac{b}{2}\right)\left(\frac{c}{2}\right)$$

where $a$, $b$, and $c$ are as defined above.

Fruit density ($\rho_{\text{fruit}}$ ; g $cm^{-3}$) was calculated using wet mass and either measured or estimated volume:

$$\rho_{\text{fruit}} = \frac{m}{V}$$

where $m$ is wet mass (g) and $V$ is fruit volume ($cm^3$) (Schön, 2015).

Total fruit surface area ($SA_{\text{total}}$; $cm^2$) was estimated using Knud Thomsen's approximation for a triaxial ellipsoid, converting axis lengths to semi-axes within the equation:

$$SA_{\text{total}} \approx 4\pi\left(\frac{\left(\left(\frac{a}{2}\right)\left(\frac{b}{2}\right)\right)^p + \left(\left(\frac{a}{2}\right)\left(\frac{c}{2}\right)\right)^p + \left(\left(\frac{b}{2}\right)\left(\frac{c}{2}\right)\right)^p}{3}\right)^{\frac{1}{p}}$$

where $p = 1.6075$ (Bestová et al., 2021; Xu et al., 2009).

Submerged *versus* emerged volume (Archimedes based).

The volume of the submerged portion of a floating fruit ($V_{\text{submerged, Arch}}$) was estimated under static equilibrium using Archimedes' principle:

$$V_{\text{submerged, Arch}} = \frac{m}{\rho_{\text{seawater}}}$$

where $m$ is fruit wet mass (g) measured after blotting excess surface water, and $\rho_{seawater}$ is seawater density. Seawater density was set to 1.027 g $cm^{-3}$, corresponding to Mediterranean seawater at 38‰ salinity and approximately 20 °C (Poulos, 2023). Emerged volume ($V_{emerged}$) was then obtained as:

$V_{\text{emerged}} = V_{\text{total}} - V_{\text{submerged, Arch}}$where $V_{total}$ is either measured by displacement (n = 41) or estimated using the triaxial ellipsoid approximation (n = 100).

### 2.4. Floating orientation experiments and dorsal protrusion characterization

Of the 41 non-frozen fruits, 18 were randomly selected to assess floating behaviour and to characterise the dorsal protrusion through excision and direct measurements. Each fruit was placed in a 2 L beaker filled with seawater at 38‰ salinity at room temperature (20–22 °C) and was dropped into the water 20 consecutive times. For each drop, a binary outcome was recorded: 0 if the fruit came to rest with the dorsal protrusion side facing up, and 1 if it settled in any other orientation. The dorsal side of each fruit was identified beforehand and marked with a small dot to facilitate visual recognition during repeated trials. Marking was applied sparingly to the exposed surface and allowed to dry before trials. A before-after check on these fruits showed that marking increased wet mass by 0.00020–0.00040 g (mean 0.00027 g; ~0.013% of fruit mass) and was therefore considered negligible for flotation and orientation outcomes.

To delineate the portion used for excision, each fruit was subsequently floated in its predominant orientation, as identified from the repeated flotation trials, and the boundary of the exposed portion above the waterline was marked. In practice, this exposed area broadly corresponded to the dorsal protrusion. The marked protrusion was then excised using a scalpel. Dorsal protrusion height (at the thickest point) and the major and minor diameters of the dorsal protrusion (Fig. 2c,d,e, f)) were measured (cm) using a digital calliper (precision 0.1 mm). The volume of dorsal protrusion was estimated following standard geometric formulations for an ellipsoidal dome. The height ($h$) of dorsal protrusion and the major and minor diameters ($d$ and $e$respectively) were measured. Diameters were converted to semi-axes ($a_{prot} = d/2$, $b_{prot} = e/2$), and the dorsal protrusion volume was calculated as:

$$V_{\text{dorsal protrusion}} = \frac{\pi h}{6}\left(3a_{prot}b_{prot} + h^2\right)$$

A dorsal protrusion-derived submerged volume estimate of fruits was computed as:

$$V_{\text{submerged, dorsal protrusion}} = V_{\text{total}} - V_{\text{dorsal protrusion}}$$

Emerged surface area ($SA_{\text{emerged}}$; $cm^2$) was estimated by approximating the dorsal protrusion as the upper half of a triaxial ellipsoid with semi-axes $a_{\text{prot}}$, $b_{\text{prot}}$ and $h$. Surface area was estimated using Knud Thomsen's approximation applied to the full ellipsoid and halved:

$$SA_{\text{emerged}} \approx 2\pi\left(\frac{(a_{prot}b_{prot})^p + (a_{prot}h)^p + (b_{prot}h)^p}{3}\right)^{1/p}$$

with $p = 1.6075$. All the dorsal protrusion dimensions were expressed in cm, yielding surface areas in $cm^2$.

### 2.5. Qualitative observations of fruit morphology

Qualitative observations of fruit structure and gross internal organisation were conducted on a separate set of 16 fruits selected from the remaining non-excised material. Longitudinal sections were made either along the dorsoventral plane or along a lateral plane orthogonal to it, and transverse sections were made perpendicular to the apico-basal axis. Multiple fruits were sectioned, and representative images were selected from the best preparations obtained. Each fruit was examined under a stereomicroscope at 160 × and 400 × magnification. Observations followed the regional division of the fruit into apical, central, and basal regions (Fig. 3a) which is similar to what was described by Celdrán and Marín (2011) for seeds of the same species.

### 2.6. Fruit dehiscence under aquarium and field conditions

Fruit dehiscence was monitored in 96 fruits under two conditions. A subset of 10 fruits was maintained in an indoor aquarium at ~20 °C and 38‰ salinity. A second group (n = 86) was placed in *ad hoc* floating arenas deployed within a sheltered marina; arenas contained fruits at the sea surface while preventing dispersal. In the field deployment, seawater temperature varied naturally, reaching ~21–22 °C during daytime and decreasing to 16–17 °C at night. Dehiscence was assessed visually as time to pericarp opening and seed release.

### 2.7. Data analyses

Fruit morphological variables were summarised using descriptive statistics (minimum, maximum, mean, standard deviation, and coefficient of variation). Floating orientation was analysed at the fruit level to account for non-independence of repeated drops. For each fruit, the proportion of trials in which the dorsal protrusion faced upward was calculated across 20 repeated drops. To test whether the predefined focal orientation occurred more frequently than all other orientations pooled together, fruit-level proportions were compared against 0.5 using a Wilcoxon signed-rank test.

The performance of the multiple linear regression model used to estimate fruit mass from the three axial measurements was assessed using $R^2$ (and adjusted $R^2$), the overall model F-test, and the significance of individual coefficients. The agreement between measured and model-estimated fruit mass was then evaluated using linear regression. Predictive performance of the triaxial ellipsoid approximation for volume was similarly evaluated using linear regressions of measured *versus* estimated values. Agreement between density estimates derived from measured and estimated volumes was assessed by regressing calculated density values against one another. Additional linear regressions were also used to examine relationships among derived fruit traits and to assess concordance among alternative estimation methods for key derived variables, including fruit mass, total volume, density, emerged volume, submerged volume, and surface area. Because several derived variables share common measurements or are mathematically linked (for example, wet mass, total volume, or axial dimensions), these analyses were interpreted primarily as comparisons of relative agreement among methods rather than as tests of independent relationships. To identify which readily measured traits best predicted more complex variables, measured fruit mass and each axis length were regressed against measured volume, density (from measured volume), estimated total surface area, emerged surface area, and submerged volume. Model fit was assessed using $R^2$, and statistical significance was evaluated at $p < 0.05$. All statistical analyses and graphical outputs were produced in R (version 4.5.1) using RStudio (version 2025.09.2 +418).

## 3. Results

### 3.1. Fruit morphology

Descriptive statistics revealed marked differences in variability among morphometric measurements and derived fruit traits (Table 1). Axial dimensions (major, intermediate, and minor axes) were relatively consistent across fruits, whereas fruit mass and volume showed greater variability. Measured and estimated values of fruit mass and total volume were broadly similar, and estimated surface area based on Knud Thomsen's equation also showed limited variation. In contrast, volume-related traits associated with floating behaviour were more heterogeneous. Submerged volumes derived from Archimedes-based calculations and emerged volumes estimated indirectly from total and submerged volume were more variable than values derived directly from dorsal protrusion measurements. By comparison, dorsal protrusion height and diameters were relatively consistent, resulting in more constrained estimates of emerged and submerged volumes when based on dorsal protrusion geometry. Across all methods, emerged volume represented approximately 18–20% of total fruit volume, indicating that a non-negligible portion of the fruit remains exposed above the water

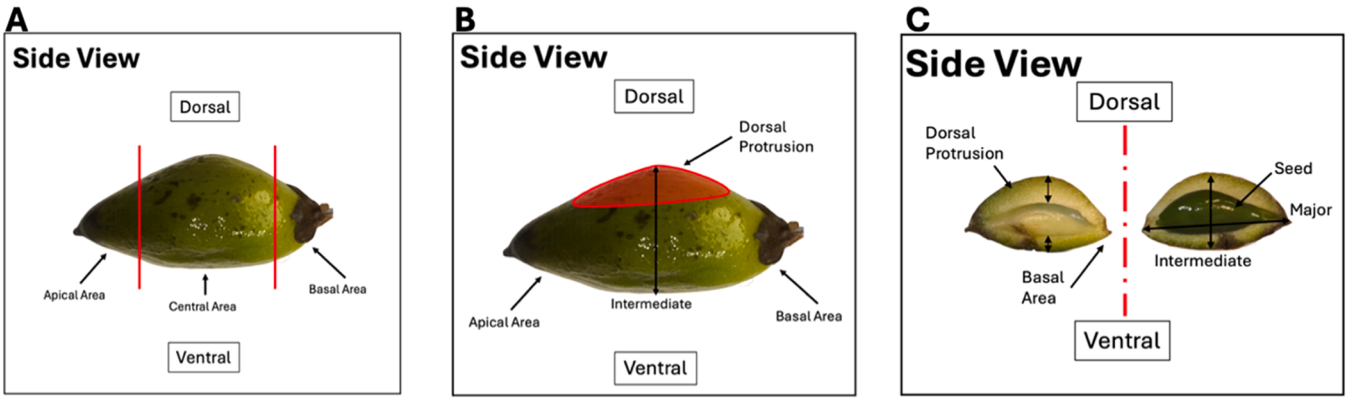


**Fig. 3.** External and internal dorsoventral asymmetry of a *Posidonia oceanica* fruit. **(a)** Lateral view of an intact fruit illustrating external morphology, dorsoventral orientation, and the apical, central, and basal regions used as a spatial framework for qualitative observations and sectioning. **(b)** Lateral view showing the dorsal protrusion, highlighted by the red outline, which extends along most of the apico-basal axis and broadly corresponds to the portion remaining above the water surface during flotation. **(c)** Longitudinal (dorsoventral) section shown as two fruit halves, illustrating internal dorsoventral asymmetry, with thicker mesocarp on the dorsal protrusion side than on the ventral side and the seed positioned closer to the ventral and basal region.

**Table 1**
Morphometric measurements, estimates, and derived calculations for *Posidonia oceanica* fruits. Values are reported as minimum (Min.), maximum (Max.), mean, standard deviation (SD), coefficient of variation (CV), and sample size (n). Superscripts indicate the method used for calculation or estimation: [a] fruit mass estimated using the multiple linear regression model based on axial measurements; [b] fruit volume estimated using the triaxial ellipsoid approximation; [c] fruit density calculated using estimated volume; [d] submerged volume calculated using Archimedes' Principle; [e] emerged volume calculated as the difference between measured total volume and submerged volume (Archimedes-based); [f] emerged volume calculated as the difference between estimated total volume and submerged volume (Archimedes-based); [g] emerged volume calculated from dorsal protrusion-derived geometric measurements; [h] submerged volume calculated from dorsal protrusion-derived emerged volume and measured total volume; [i] emerged surface area estimated by approximating the dorsal protrusion as the upper half of a triaxial ellipsoid (Knud Thomsen's approximation).

| Measure | Min. | Max. | Mean | SD | CV (%) | n |
|---|---|---|---|---|---|---|
| Major axis (cm) | 1.90 | 3.11 | 2.72 | 0.24 | 8.81 | 100 |
| Intermediate axis (cm) | 0.98 | 1.59 | 1.32 | 0.12 | 8.74 | 100 |
| Minor axis (cm) | 0.95 | 1.48 | 1.24 | 0.10 | 8.30 | 100 |
| Mass (g) | 0.761 | 2.729 | 1.943 | 0.39 | 19.771 | 100 |
| Mass[a] (g) | 0.642 | 2.625 | 1.956 | 0.34 | 17.653 | 100 |
| Volume ($cm^3$) | 1.30 | 3.30 | 2.33 | 0.44 | 18.75 | 41 |
| Volume[b] ($cm^3$) | 0.93 | 3.53 | 2.35 | 0.48 | 20.58 | 100 |
| Density ($g/cm^3$) | 0.75 | 0.92 | 0.84 | 0.04 | 4.97 | 41 |
| Density[c] ($g/cm^3$) | 0.66 | 0.93 | 0.83 | 0.05 | 6.61 | 100 |
| Surface area ($cm^2$) | 4.93 | 12.07 | 9.29 | 1.28 | 13.83 | 100 |
| Submerged volume[d] ($cm^3$) | 0.74 | 2.66 | 1.89 | 0.37 | 19.77 | 100 |
| Emerged volume[e] ($cm^3$) | 0.21 | 0.74 | 0.42 | 0.13 | 31.27 | 41 |
| Emerged volume[f] ($cm^3$) | 0.19 | 0.98 | 0.46 | 0.18 | 39.03 | 100 |
| Dorsal protrusion height (cm) | 0.55 | 0.60 | 0.56 | 0.02 | 4.09 | 18 |
| Major diameter of dorsal protrusion (cm) | 1.12 | 1.75 | 1.43 | 0.21 | 14.95 | 18 |
| Minor diameter of dorsal protrusion (cm) | 0.95 | 1.44 | 1.16 | 0.15 | 12.81 | 18 |
| Emerged volume[g] ($cm^3$) | 0.37 | 0.58 | 0.46 | 0.06 | 12.05 | 18 |
| Submerged volume[h] ($cm^3$) | 1.54 | 2.60 | 1.92 | 0.30 | 15.80 | 18 |
| Emerged surface area ($cm^2$)[i] | 2.01 | 2.84 | 2.40 | 0.23 | 9.79 | 18 |

surface during flotation.

### 3.2. Qualitative observations

Qualitative observations revealed marked dorsoventral asymmetry in fruit morphology. In lateral view, fruits exhibited a continuous dorsal protrusion extending from the basal to the apical region, producing a strongly convex dorsal surface and a comparatively flatter ventral side (Fig. 3b). Maximum fruit height coincides with this protrusion, providing a clear external reference for subsequent flotation-related measurements.

Longitudinal sections along the apico-basal (major) axis confirmed internal dorsoventral asymmetry, with mesocarp thickness substantially greater on the dorsal protrusion side than on the ventral side (Fig. 3c). By contrast, longitudinal sections taken in a lateral plane orthogonal to the dorsoventral axis showed broadly symmetric mesocarp thickness across the two lateral sides (Fig. 4a). Across sections, the seed was consistently positioned closer to the basal and ventral portions of the fruit.

Transverse sections perpendicular to the apico-basal axis revealed a distinct longitudinal groove on the dorsal surface of the seed. This groove corresponded to the dorsally thickened mesocarp region aligned with the external dorsal protrusion (Fig. 4b). Serial transverse sections further indicated that this dorsoventral differentiation was spatially localised, being most pronounced in the central region containing the seed and progressively less evident toward the apical and basal ends.

The dorsal groove extended along the apico-basal axis of the seed (Fig. 5a). After seed removal, the fruit's inner concave surface was fully exposed. In the dorsal half, a distinct pale-yellow, lens-shaped structure was consistently present. It was soft and pliable, with a faint granular appearance and scattered translucent inclusions (Fig. 5b). This structure was not attached to the seed but rested against the inner mesocarp and closely matched the position of the seed's dorsal groove. A subtle strand-like continuity toward the basal end was visible in all examined fruits, suggesting a possible connection near the pedicel insertion. In the opposite (ventral) half, the corresponding region lacked the pale-yellow tissue and instead appeared as a continuous linear ridge on the inner mesocarp surface. Additional images of the pale-yellow structure and dorsoventral asymmetry are provided in Figs. S1-S3 of the Supplementary Materials.

### 3.3. Fruit floating behaviour

Fruit buoyancy orientation showed a strong preference for the dorsal protrusion facing upward. Across 360 repeated drops, fruits came to rest in this focal orientation in 306 cases (85% overall), compared with 54 cases (15%) in all other orientations combined (Fig. S4). At the fruit level, the frequency of dorsal-protrusion-up orientation ranged from 10% to 100%, with a median value of 90% (Fig. S4). In 17 of the 18 fruits, the dorsal protrusion faced upward in at least 70% of trials (Fig. S4). A Wilcoxon signed-rank test comparing fruit-level proportions against 0.5 confirmed that this focal orientation occurred significantly more often than the pooled alternative orientations ($W = 10.5$, $p = 0.00042$).

### 3.4. Validation of estimates

Fruit mass was strongly predicted by axial dimensions using the multiple linear regression model based on the three fruit axes (major, intermediate and minor) (Table 2). All three predictors contributed positively and significantly to the model, and the resulting estimates closely matched measured fruit mass (Table 2).

The table reports the fitted model equation, a) overall model fit statistics, and b) regression coefficients for the three axial predictors (major, intermediate, and minor axes). Regression equations, coefficients of determination ($R^2$), F-values, degrees of freedom (df), and p-values are reported.

Fruit mass estimated from axial measurements closely matched measured fruit mass, and measured fruit volume was similarly well approximated by the triaxial ellipsoid model (Table 3; Figs. S5-S6). In contrast, density estimates derived from measured and estimated volumes showed little correspondence, and emerged-volume estimates obtained using different approaches were only weakly related (Table 3; Figs. S7-S9). By comparison, submerged volume estimated using Archimedes' principle showed a close agreement with values derived from the dorsal protrusion measurements (Table 3; Fig. S10). Overall, concordance was stronger for total and submerged volume than for emerged-volume estimates.

Measured fruit mass was strongly related to fruit volume and estimated surface area, whereas its relationships with fruit density and emerged surface area were weaker (Table 4; Figs. S12-S14).

The major axis showed a moderate relationship with fruit mass, whereas the strongest relationships were observed for the intermediate and minor axes. The same pattern was found for fruit volume and submerged volume estimated using Archimedes' principle (Table 5; Figs. S15–S25). In contrast, emerged surface area, dorsal protrusion height, and dorsal protrusion diameters showed little or no relationship with axial measurements.

### 3.5. Fruit dehiscence

Under aquarium conditions, fruit dehiscence occurred between 11 and 16 days after collection. Specifically, two fruits dehisced after 11 days, one after 12 days, four after 14 days, two after 15 days, and one

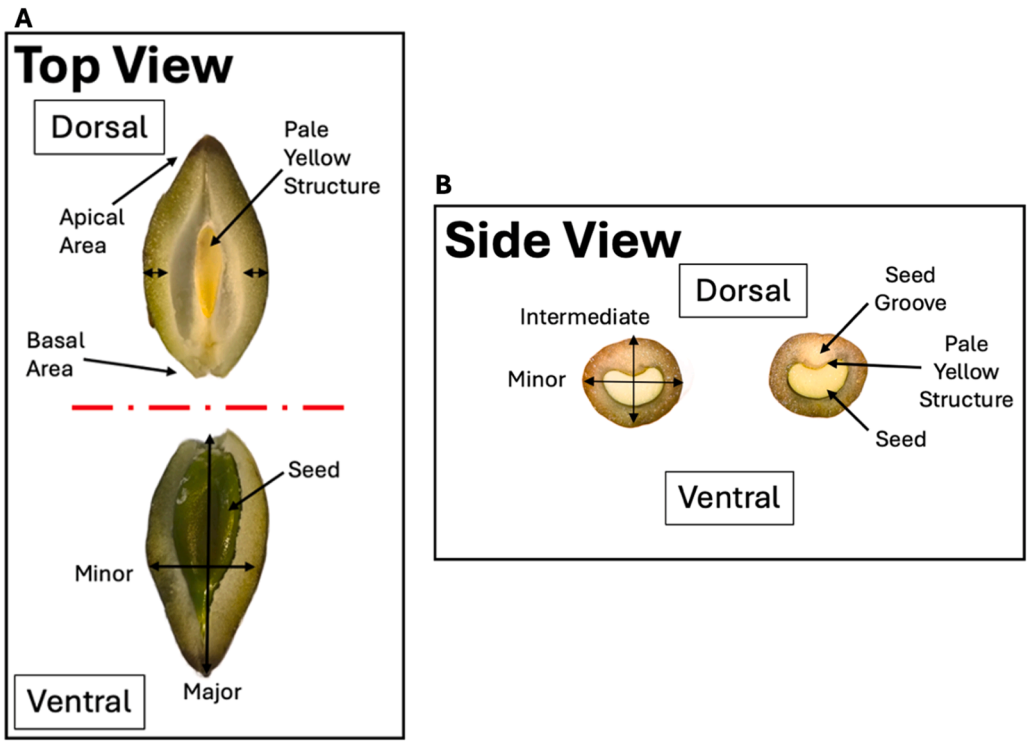


**Fig. 4.** Internal organisation of a *Posidonia oceanica* fruit in longitudinal and transverse sections. **(a)** Longitudinal section along a lateral plane orthogonal to the dorsoventral axis, exposing the seed in situ and showing broadly symmetrical mesocarp thickness on the two lateral sides of the fruit. **(b)** Representative transverse sections perpendicular to the apico-basal axis. The section containing the seed shows the seed groove, the pale-yellow structure, and pronounced dorsoventral differences in tissue thickness, whereas the section away from the seed-bearing central region is comparatively more symmetrical.

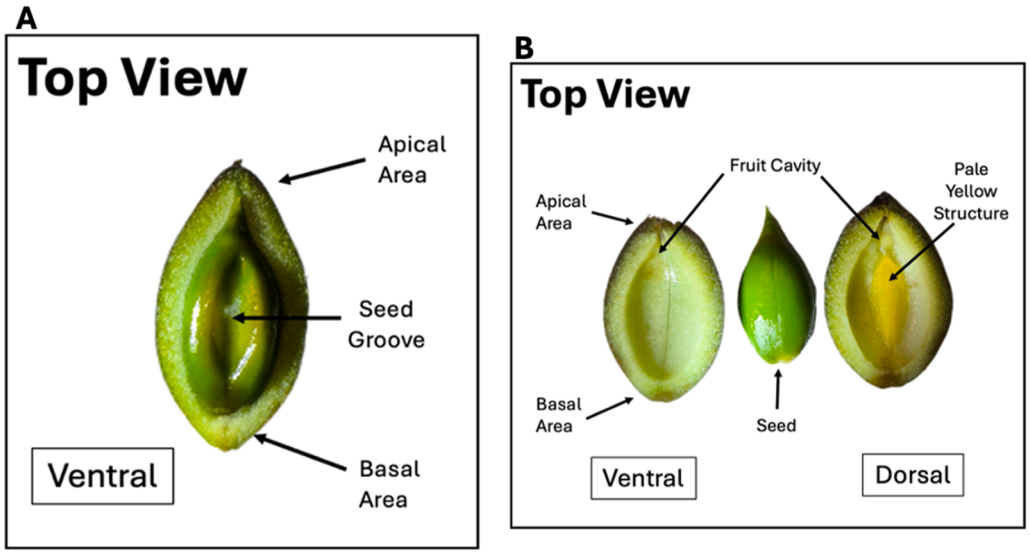


**Fig. 5.** Relationship between the seed groove and the pale-yellow structure in *Posidonia oceanica* fruits. **(a)** Top view of an isolated seed showing a distinct longitudinal groove extending along the apico-basal axis. **(b)** Fruit opened longitudinally, showing the seed and the concave inner surfaces of the mesocarp halves. A pale-yellow lenticular structure is visible along the dorsal inner surface and aligns with the seed groove shown in **(a)**. The corresponding region on the ventral half lacks this pale-yellow tissue and instead appears as a continuous linear ridge on the inner mesocarp surface.

after 16 days. In the field-based floating arenas, no fruits dehisced within the first 14 days of observation. Field observations were terminated after 14 days because of storm-related damage to the deployment infrastructure.

## 4. Discussion

Sexual reproduction and fruit-mediated dispersal can contribute to genetic diversity, connectivity, and the long-term persistence of *Posidonia oceanica* meadows, yet the physical determinants of fruit transport at the sea surface remain less well understood than phenology, recruitment, and seed traits (Balestri and Cinelli, 2003; Belzunce et al.,

**Table 2**
Multiple linear regression model predicting fruit mass from axial measurements.

**a)**

| Predictor | Response | n | $R^2$ | F-value | Df | p-value |
|---|---|---|---|---|---|---|
| Major, intermediate, and minor axes | Fruit mass (g) | 100 | 0.86 | 190.07 | 3,96 | < 0.001 |

**b)**

| Term | Coefficient | SE | t-value | p-value |
|---|---|---|---|---|
| Intercept | −2.865 | 0.2 | −13.94 | < 0.001 |
| Major axis | 0.827 | 0.1 | 12.6 | < 0.001 |
| Intermediate axis | 1.159 | 0.3 | 4.03 | < 0.001 |
| Minor axis | 0.842 | 0.3 | 2.62 | 0.01 |

**Table 3**
Validation of fruit morphology estimates. Linear regressions comparing directly measured fruit traits with corresponding values estimated from axial measurements, geometric approximations, or Archimedes-based calculations. For each model, the regression equation, $R^2$, F statistic, degrees of freedom, and p-value are reported. Analyses were conducted on the relevant subsets of fruits (n = 100 for mass-based comparisons, n = 41 for traits requiring measured volume, and n = 18 for comparisons involving dorsal protrusion-derived measurements). Variable codes identify whether each trait was measured directly or estimated from regression, geometry, or Archimedes-based calculations: [a], measured fruit mass; [b], estimated fruit mass from multiple regression; [c], measured fruit volume (water displacement); [d], fruit volume estimated using the triaxial ellipsoid approximation; [e], fruit density calculated using measured volume; [f], fruit density calculated using estimated volume; [g], emerged volume calculated using Archimedes' principle and measured total volume; [h], emerged volume calculated using Archimedes' principle and estimated total volume; [i], emerged volume calculated from dorsal protrusion-derived measurements; [j], submerged volume calculated from dorsal protrusion-derived measurements and measured total volume; [k], submerged volume calculated using Archimedes' principle. Regression equations, coefficients of determination ($R^2$), F-values, degrees of freedom (df), and p-values are reported.

| Predictor | Response | Regression Equation | n | $R^2$ | F-value | Df | p-value |
|---|---|---|---|---|---|---|---|
| Mass[a] | Mass[b] | y = 0.843x + 0.317 | 100 | 0.88 | 723.5 | 1,98 | < 0.001 |
| Volume[c] | Volume[d] | y = 1.007x + 0.071 | 41 | 0.87 | 252.3 | 1,39 | < 0.001 |
| Density[e] | Density[f] | y = 0.2x + 0.647 | 41 | 0.02 | 0.994 | 1,39 | 0.340 |
| Emerged Volume[g] | Emerged Volume[h] | y = 0.554x + 0.273 | 41 | 0.17 | 7.756 | 1,39 | 0.008 |
| Emerged Volume[g] | Emerged Volume[i] | y = 0.14x + 0.396 | 18 | 0.08 | 1.298 | 1,16 | 0.271 |
| Submerged Volume[j] | Submerged Volume[k] | y = 0.82x + 0.365 | 18 | 0.88 | 117.3 | 1,16 | < 0.001 |

**Table 4**
Linear regression analyses between measured fruit mass and selected morphological traits, including fruit volume, density, estimated surface area, and emerged surface area. Regression equations, coefficients of determination ($R^2$), F-values, degrees of freedom (df), and p-values are reported. Superscripts indicate the method used for calculation or estimation: [a] measured; [b] calculated using measured volume; [c] estimated using Knud Thomsen's equation; [d] emerged surface area estimated by approximating the dorsal protrusion as the upper half of a triaxial ellipsoid using Knud Thomsen's approximation ($p = 1.6075$).

| Predictor | Response | Regression Equation | N | $R^2$ | F-value | Df | p-value |
|---|---|---|---|---|---|---|---|
| Mass | Volume[a] | y = 1.138x + 0.097 | 41 | 0.93 | 513.8 | 1,39 | < 0.001 |
| Mass | Density[b] | y = 0.025x + 0.794 | 41 | 0.05 | 1.971 | 1,39 | 0.168 |
| Mass | Surface Area[c] | y = 3.158x + 3.148 | 100 | 0.89 | 817.9 | 1,98 | < 0.001 |
| Mass | Emerged Surface Area[d] | y = 0.19x + 2.03 | 18 | 0.05 | 0.793 | 1,16 | 0.386 |

**Table 5**
Linear regression analyses between fruit axes (major, intermediate, and minor axes) and morphological traits, including fruit mass, volume, surface area, and submerged volume. Regression equations, coefficients of determination ($R^2$), F-values, degrees of freedom (df), and p-values are reported. Superscripts indicate the method used for calculation or estimation: [a] measured fruit mass; [b] measured fruit volume; [c] estimated using Knud Thomsen's equation; [d] calculated using Archimedes' Principle. Fruit surface area is included as a geometry-derived descriptor estimated from axial measurements and is therefore not independent of the predictors.

| Predictor | Response | Regression Equation | n | $R^2$ | F-value | Df | p-value |
|---|---|---|---|---|---|---|---|
| Major Axis | Mass[a] | y = 0.123x−1.107 | 100 | 0.49 | 93.97 | 1,98 | < 0.001 |
| Intermediate Axis | Mass[a] | y = 2.789x−1.745 | 100 | 0.70 | 232.4 | 1,98 | < 0.001 |
| Minor Axis | Mass[a] | y = 3.171x−1.979 | 100 | 0.72 | 248.5 | 1,98 | < 0.001 |
| Major Axis | Volume[b] | y = 1.186x−0.943 | 41 | 0.40 | 26.04 | 1,39 | < 0.001 |
| Intermediate Axis | Volume[b] | y = 3.643x−2.515 | 41 | 0.75 | 118.8 | 1,39 | < 0.001 |
| Minor Axis | Volume[b] | y = 3.664x−2.232 | 41 | 0.70 | 92.55 | 1,39 | < 0.001 |
| Major Axis | Surface Area[c] | y = 4.254x−2.266 | 100 | 0.63 | 165.7 | 1,98 | < 0.001 |
| Intermediate Axis | Surface Area[c] | y = 9.508x−3.287 | 100 | 0.73 | 267.2 | 1,98 | < 0.001 |
| Minor Axis | Surface Area[c] | y = 10.513x - 3.719 | 100 | 0.71 | 235 | 1,98 | < 0.001 |
| Major Axis | Submerged Volume[d] | y = 1.094x−1.078 | 100 | 0.49 | 93.97 | 1,98 | < 0.001 |
| Intermediate Axis | Submerged Volume[d] | y = 2.716x−1.699 | 100 | 0.70 | 232.4 | 1,98 | < 0.001 |
| Minor Axis | Submerged Volume[d] | y = 3.088x−1.927 | 100 | 0.72 | 248.5 | 1,98 | < 0.001 |

2005; Kendrick et al., 2012). Here, we link external morphology, internal organisation and flotation behaviour to identify traits that are directly relevant to near-surface transport. Our main result is that dorsoventral asymmetry is associated with stable floating orientation and a reproducible emerged fraction under the static conditions tested here. This emerged fraction may therefore serve as an empirical trait in future dispersal and connectivity models, rather than being assumed arbitrarily. Axial dimensions varied relatively little among fruits, whereas mass- and volume-related traits were more variable. This pattern does not imply inconsistency in the measurements, because

volume depends on the combined product of all three axes and therefore amplifies moderate variation across dimensions. In addition, displacement-based volume reflects the actual fruit shape, whereas the triaxial ellipsoid approximation simplifies that shape and does not fully capture deviations such as dorsal asymmetry. Because fruits were selected using clear indicators of freshness and processed rapidly, the observed variability more plausibly reflects biological and structural differences than artefacts of handling. Conversely, fruit density varied comparatively little, supporting buoyancy maintenance as a robust property during the surface phase. This interpretation is consistent with histological evidence for low-density, lacunar tissues in *P. oceanica* fruit pericarps (Pinna et al., 2026). However, the duration and conditions of surface transport prior to stranding cannot be quantified and may have contributed to among-fruit variability.

A central finding is that fruit dorsoventral asymmetry is consistently associated with stable floating orientation. Fruits possess a continuous dorsal protrusion, and replicated drop trials showed a strong tendency to self-orient with this dorsal side facing upward. Rather than suggesting active "steering", these results are more consistent with a hydrostatic interpretation in which asymmetry may favour a preferred floating equilibrium. In turn, this stabilises the portion of the fruit exposed above the waterline, making surface exposure—and therefore potential windage—more predictable during transport at the air-sea interface. Across methods, the emerged fraction was consistently around 18–20% of total fruit volume, indicating that this exposed component is a repeatable trait of the floating phase. Even modest exposure can influence drift by increasing sensitivity to wind forcing, which has been documented for floating debris and for biological propagules in other systems (Maximenko et al., 2012; van der Stocken et al., 2015). Recent trait-based biophysical modelling further supports the idea that variability in buoyancy and windage among propagules can translate into large differences in dispersal distance and direction (Hanuise et al., 2025). Our results may help reduce an important source of uncertainty in near-surface dispersal modelling, because windage depends on posture at the air-sea interface. Because *P. oceanica* fruits adopt a repeatable floating posture, the proportion of the fruit exposed above the waterline can be treated as a constrained trait rather than an unconstrained assumption. This provides an empirical parameter for dispersal models and reduces reliance on *ad hoc* tuning. This is particularly relevant for *P. oceanica*, because recent Mediterranean-wide biophysical modelling shows that floating duration strongly shapes potential connectivity, while direct wind drag on floating fruits is not separately parameterised (Barrier et al., 2026).

The ecological relevance of stable exposure depends on the duration of the surface phase prior to seed release. Under aquarium conditions, fruits dehisced between 11 and 16 days after collection, whereas in sheltered field floating arenas no fruits dehisced within the first 14 days (the trial ended early due to storm-related damage). This contrast is most plausibly interpreted as environmental modulation of dehiscence rather than a discrepancy between datasets. Although the underlying drivers were not tested directly, several differences between the two settings may have contributed, including the more stable thermal regime in the aquarium, the stronger day–night temperature fluctuations in the field deployment, and other uncontrolled differences in physical conditions at the fruit surface. Treating dehiscence time as a range is consistent with descriptions of *P. oceanica* sexual recruitment as a sequence of stages that includes a surface dispersal phase in intact fruits (Guerrero-Meseguer et al., 2018). Available accounts of the surface phase are often qualitative, spanning from "a few days" (Belzunce et al., 2005) to "days to weeks" in broader syntheses (e.g., McMahon et al., 2014; André et al., 2023), and inference from collected or beach-cast fruits is further complicated by uncertainty in detachment timing (Ruocco et al., 2025). A stable orientation trait remains valuable because it provides a baseline estimate for surface exposure across plausible surface-phase durations. Comparable wind-current coupling during surface dispersal has been documented for floating fruits of *P. australis*, where both surface currents and direct wind forcing contribute to transport trajectories and potential connectivity patterns (Ruiz-Montoya et al., 2012). Similar processes are expected to influence connectivity in Mediterranean *P. oceanica* meadows, where basin-scale simulations indicate that dispersal trajectories can link distant populations through surface transport pathways (Mari et al., 2020). For eelgrass (*Zostera marina*), long-distance dispersal can occur via floating reproductive shoots, and modelling approaches often include an explicit wind-drag component to represent near-surface transport, again emphasising that partial emergence and exposure can matter even when the propagule type differs (Erftemeijer et al., 2008; see also Källström et al., 2008).

In *P. oceanica* fruits, macroscopic sectioning showed that the external dorsal protrusion corresponds to a consistent internal dorsoventral organisation. The region underlying the dorsal protrusion corresponds to increased dorsal mesocarp thickness above the seed and aligns with a longitudinal groove on the dorsal seed surface. A pale-yellow, soft and pliable structure observed in the dorsal portion of the fruit cavity corresponded with the seed groove, whereas the ventral half lacked this structure and instead showed a ridge-like feature along the inner mesocarp surface. The repeatability and spatial specificity of these features suggest that dorsoventral asymmetry is not merely superficial but reflects a coherent internal architecture that could contribute to stability through buoyant tissue distribution and/or mass arrangement around the seed. An additional, non-exclusive possibility is that dorsal and ventral regions differ not only in volume but also in tissue density, for example through differences in sponginess or lacunar development, which could further influence floating equilibrium. Recent histological evidence for low-density, lacunar tissues in *P. oceanica* fruit pericarps supports the plausibility of this mechanism, although dorsoventral differences in tissue density were not tested here (Pinna et al., 2026).

At this stage, however, tissue identity and functional contribution remain hypotheses because observations are macroscopic. A distinct integumentary outgrowth has previously been described in the genus *Posidonia*, where it originates from the fused integuments and lies opposite the micropyle (Remizowa et al., 2012). By contrast, the pale-yellow structure observed here was documented macroscopically in mature fruits, and its tissue identity, developmental origin, and homology remain unresolved. Histological and compositional work will therefore be needed to test whether the seed-groove-associated structure contributes to buoyancy, stability or seed physiology. In a strictly functional sense, and without implying homology, the descriptor "aril-like" can be used provided that this limitation is made explicit (Endress, 1973; Borsch et al., 2008; Povilus et al., 2015). These observations help describe the floating fruit phase in physical terms, which in the *P. oceanica* literature has often remained qualitative. By quantifying orientation stability, emerged fraction and practical proxies, the present work helps to connect recruitment-stage descriptions of the fruit phase to trait-informed dispersal modelling.

Evidence from other hydrochorous systems suggests that floating orientation and surface exposure can influence the sensitivity of dispersal to wind forcing. In mangrove propagules, for example, wind-driven transport depends on propagule morphology and the fraction exposed at the surface (van der Stocken et al., 2013; van der Stocken et al., 2019), while similar effects of wind on floating seeds have been documented in slow-flowing or stagnant water bodies (Sarneel et al., 2014). Within this broader physical context, the stable orientation and reproducible emerged fraction of *P. oceanica* fruits are likely to influence how they respond to combined wind and current forcing during surface dispersal. Our results also show which dispersal-relevant traits can be estimated most reliably from simple measurements. The close agreement between measured and estimated mass and total volume supports the use of regression- and geometry-based proxies as practical indirect estimates, particularly when only axial measurements are available or when direct weighing and volumetric measurements are impractical (Koc, 2007; Khojastehnazhand et al., 2010; Neupane et al., 2023). Mass was strongly related to volume and to estimated total surface area,

consistent with mass-based approximations reported for other biological objects (Eifert et al., 2006). By contrast, the weaker agreement among emerged-volume estimates than among submerged-volume estimates indicates greater sensitivity to how the trait is derived. In the present dataset, emerged volume was obtained either as a difference between total and submerged volume or from dorsal protrusion-based geometry, making it more sensitive to cumulative measurement error and to assumptions about protrusion shape and the air–water interface. In practice, total and submerged volume appear to be the most robust proxy-based descriptors, whereas emerged-fraction estimates are more sensitive to method choice and would benefit from image-based or 3D approaches. Despite increasing interest in seagrass connectivity, quantitative descriptions of the physical traits controlling the surface phase of floating fruits remain scarce for *P. oceanica*.

Overall, dorsoventral asymmetry provides a consistent morphological basis for stable floating orientation in *P. oceanica* fruits, and the emerged fraction estimated here offers a tractable parameter for near-surface transport. Beyond dispersal modelling, these results provide a baseline for comparative studies of fruit functional morphology, dispersal ecology, connectivity, and restoration-oriented research. However, buoyancy and orientation trials were conducted under static laboratory conditions and did not incorporate wind or current forcing, so the stability documented here should be treated as a baseline property that still requires validation under dynamic regimes. In addition, surface area was estimated using analytical approximations based on simplified geometry rather than measured directly. Future work should combine anatomical validation with controlled hydrodynamic experiments including wind and current forcing and could further reduce uncertainty through 3D scanning or photogrammetry alongside the geometric proxies presented here.

## Conclusion

This study shows that dorsoventral asymmetry provides a consistent morphological basis for stable floating orientation in *Posidonia oceanica* fruits. By linking external morphology, internal organisation, and flotation behaviour, it identifies a reproducible emerged fraction and practical proxy-based descriptors of the floating phase that can support a more quantitative description of near-surface dispersal. Beyond improving trait-informed dispersal modelling, these results provide baseline information for future studies of dispersal ecology, connectivity, comparative fruit functional morphology, and restoration-oriented research in seagrasses.

## Author contributions

TL and FB conceived the study, carried out the measurements and data analyses, and drafted the manuscript. CP assisted with selected measurements. AZ contributed to the estimates based on Archimedes' principle. AA, MM and AZ contributed to the field experiments on fruit dehiscence. All authors reviewed, revised, and approved the final manuscript.

## CRediT authorship contribution statement

**Trace Laskey:** Writing – original draft, Investigation, Formal analysis, Data curation, Conceptualization. **Fabio Badalamenti:** Writing – review & editing, Writing – original draft, Project administration, Methodology, Investigation, Funding acquisition, Formal analysis, Data curation, Conceptualization. **Carlo Pipitone:** Writing – review & editing. **Marco Martinez:** Writing – review & editing, Investigation. **Infantes eduardo:** Writing – review & editing. **Vincenzo Maximiliano Giacalone:** Writing – review & editing. **D'Anna Giovanni:** Writing – review & editing. **Alagna adriana:** Writing – review & editing, Investigation. **Arturo Zenone:** Writing – review & editing, Methodology, Investigation.

## Ethics Approval

The article does not contain any studies with animals performed by any of the authors.

## Funding

This study was supported by funds provided under the National Recovery and Resilience Plan (NRRP), Mission 4 Component 2 Investment 1.4 - Call for tender No. 3138 of 16 December 2021, rectified by Decree n.3175 of 18 December 2021 of the Italian Ministry of University and Research funded by the European Union - NextGenerationEU. Project code CN_00000033, Concession Decree No. 1034 of 17 June 2022 adopted by the Italian Ministry of University and Research, CUP B83C22002930006 (CNR), Project title "National Biodiversity Future Center- NBFC''.

## Declaration of Competing Interest

The authors declare that they have no conflict of interest.

## Acknowledgments

We would like to thank Raphael Da Silveira Bueno and Silvio Fici for their help in describing the internal fruit morphology.

## Appendix A. Supporting information

Supplementary data associated with this article can be found in the online version at doi:10.1016/j.aquabot.2026.104047.

## Data availability

we are submitting a data in brief paper, data will be aivalaible later.

## References

André, S., Astruch, P., Boudouresque, C.-F., Belloni, B., Bardinal, V., Boada, J., Charbonnel, É., Chéré, E., Cottalorda, J.-M., Estaque, T., Ferrari, B., Guillemain, D., Hartmann, V., Hubert, R., Jamme, S., Lazennec, A., Michez, N., Molenaar, H., Monnier, B., Pergent, G., Pergent-Martini, C., Pey, A., Schohn, T., Teixidó, N., 2023. The 2022 mass flowering of *Posidonia oceanica* in the French Mediterranean Sea: is it unprecedented? Sci. Rep. Port. -Cros Natl. Park. 37, 65–100.

Balestri, E., Cinelli, F., 2003. Sexual reproductive success in *Posidonia oceanica*. Aquat. Bot. 75, 21–32. https://doi.org/10.1016/S0304-3770(02)00151-1.

Barrier, C., Durieux, É.D.H., Pasqualini, V., Astruch, P., Monnier, B., 2026. Biophysical modeling of *Posidonia oceanica* fruit dispersal in the Mediterranean Sea. Mar. Environ. Res. 220, 108126. https://doi.org/10.1016/j.marenvres.2026.108126.

Belzunce, M., Navarro, R.M., Rapoport, H.F., 2005. Seed and early plantlet structure of the Mediterranean seagrass *Posidonia oceanica*. Aquat. Bot. 82, 269–283. https://doi.org/10.1016/j.aquabot.2005.04.006.

Bestová, H., Segrestin, J., von Schwartzenberg, K., Škaloud, P., Lenormand, T., Violle, C., 2021. Biological scaling in green algae: the role of cell size and geometry. Sci. Rep. 11, 14425. https://doi.org/10.1038/s41598-021-93816-2.

Borsch, T., Löhne, C., Wiersema, J., 2008. Phylogeny and evolutionary patterns in Nymphaeales: integrating genes, genomes and morphology. Taxon 57, 1052–1081. https://doi.org/10.1002/tax.574004.

Celdrán, D., Marín, A., 2011. Photosynthetic activity of the non-dormant *Posidonia oceanica* seed. Mar. Biol. 158, 853–858. https://doi.org/10.1007/s00227-010-1612-4.

Duarte, C.M., Agusti, S., Barbier, E., Britten, G.L., Castilla, J.C., Gattuso, J.-P., Fulweiler, R.W., Hughes, T.P., Knowlton, N., Lovelock, C.E., Lotze, H.K., Predragovic, M., Poloczanska, E., Roberts, C., Worm, B., 2020. Rebuilding marine life. Nature 580, 39–51. https://doi.org/10.1038/s41586-020-2146-7.

Eifert, J.D., Sanglay, G.C., Lee, D.J., Sumner, S.S., Pierson, M.D., 2006. Prediction of raw produce surface area from weight measurement. J. Food Eng. 74, 552–555. https://doi.org/10.1016/j.jfoodeng.2005.02.030.

Endress, P.K., 1973. Arils and aril-like structures in woody Ranales. New. Phytol. 72, 1159–1171. https://doi.org/10.1111/j.1469-8137.1973.tb02092.x.

Erftemeijer, P.L.A., van Beek, J.K.L., Ochieng, C.A., Jager, Z., Los, H.J., 2008. Eelgrass seed dispersal via floating generative shoots in the Dutch Wadden Sea: a model approach. Mar. Ecol. Prog. Ser. 358, 115–124. https://doi.org/10.3354/meps07304.

Fourqurean, J.W., Duarte, C.M., Kennedy, H., Marbà, N., Holmer, M., Mateo, M.A., Apostolaki, E.T., Kendrick, G.A., Krause-Jensen, D., McGlathery, K.J., Serrano, O.,

2012. Seagrass ecosystems as a globally significant carbon stock. Nat. Geosci. 5, 505–509. https://doi.org/10.1038/ngeo1477.
Grech, A., Wolter, J., Coles, R., McKenzie, L., Rasheed, M., Thomas, C., Waycott, M., Hanert, E., 2016. Spatial patterns of seagrass dispersal and settlement. Divers. Distrib. 22, 1150–1162. https://doi.org/10.1111/ddi.12479.
Guerrero-Meseguer, L., Sanz-Lázaro, C., Marín, A., 2018. Understanding the sexual recruitment of one of the oldest and largest organisms on Earth, the seagrass *Posidonia oceanica*. PLoS. One 13, e0207345. https://doi.org/10.1371/journal.pone.0207345.
Hanuise, D., Dobbelaere, T., Choukroun, S., Rasheed, M.A., Lambrechts, J., York, P.H., Smith, T.M., Coles, R.G., Hanert, E., Grech, A., 2025. Integrating interspecific traits into biophysical models of seagrass dispersal. Ecol. Model. 510, 111329. https://doi.org/10.1016/j.ecolmodel.2025.111329.
Infantes, E., Orfila, A., Bouma, T.J., Simarro, G., Terrados, J., 2011. *Posidonia oceanica* and *Cymodocea nodosa* seedling tolerance to wave exposure. Limnol. Oceanogr. 56, 2223–2232. https://doi.org/10.4319/lo.2011.56.6.2223.
Infantes, E., Orfila, A., Simarro, G., Luhar, M., Terrados, J., Nepf, H., 2012. Effect of a seagrass (*Posidonia oceanica*) meadow on wave propagation. Mar. Ecol. Prog. Ser. 456, 63–72. https://doi.org/10.3354/meps09754.
Jahnke, M., Casagrandi, R., Melià, P., Schiavina, M., Schultz, S.T., Zane, L., Procaccini, G., 2017. Potential and realized connectivity of the seagrass *Posidonia oceanica* and their implication for conservation. Divers. Distrib. 23, 1423–1434. https://doi.org/10.1111/ddi.12633.
Källström, B., Nyqvist, A., Åberg, P., Bodin, M., André, C., 2008. Seed rafting as a dispersal strategy for eelgrass (*Zostera marina*). Aquat. Bot. 88, 148–153. https://doi.org/10.1016/j.aquabot.2007.09.005.
Kendrick, G.A., Waycott, M., Carruthers, T.J.B., Cambridge, M.L., Hovey, R., Krauss, S.L., Lavery, P.S., Les, D.H., Lowe, R.J., Vidal, O.M., Ooi, J.L.S., Orth, R.J., Rivers, D.O., Ruiz-Montoya, L., Sinclair, E.A., Statton, J., van Dijk, J.K., Verduin, J.J., 2012. The central role of dispersal in the maintenance and persistence of seagrass populations. Bioscience 62, 56–65. https://doi.org/10.1525/bio.2012.62.1.10.
Khojastehnazhand, M., Omid, M., Tabatabaeefar, A., 2010. Determination of tangerine volume using image processing methods. Int. J. Food Prop. 13, 760–770. https://doi.org/10.1080/10942910902894062.
Koc, A.B., 2007. Determination of watermelon volume using ellipsoid approximation and image processing. Postharvest Biol. Technol. 45, 366–371. https://doi.org/10.1016/j.postharvbio.2007.03.010.
Mari, L., Melià, P., Fraschetti, S., Gatto, M., Casagrandi, R., 2020. Spatial patterns and temporal variability of seagrass connectivity in the Mediterranean Sea. Divers. Distrib. 26, 169–182. https://doi.org/10.1111/ddi.12998.
Maximenko, N., Hafner, J., Niiler, P., 2012. Pathways of marine debris derived from trajectories of Lagrangian drifters. Mar. Pollut. Bull. 65, 51–62. https://doi.org/10.1016/j.marpolbul.2011.04.016.
McMahon, K., van Dijk, K.J., Ruiz-Montoya, L., Kendrick, G.A., Krauss, S.L., Waycott, M., Verduin, J., Lowe, R., Statton, J., Brown, E., Duarte, C., 2014. The movement ecology of seagrasses. Proc. R. Soc. B 281, 20140878. https://doi.org/10.1098/rspb.2014.0878.
Moreira-Saporiti, A., Teichberg, M., Garnier, E., Cornelissen, J.H.C., Alcoverro, T., Björk, M., Boström, C., Dattolo, E., Eklöf, J.S., Hasler-Sheetal, H., Marbà, N., Marín-Guirao, L., Meysick, L., Olivé, I., Reusch, T.B.H., Ruocco, M., Silva, J., Sousa, A.I., Procaccini, G., Santos, R., 2023. A trait-based framework for seagrass ecology: trends and prospects. Front. Plant. Sci. 14, 1088643. https://doi.org/10.3389/fpls.2023.1088643.
Neupane, C., Pereira, L., Koirala, A., Walsh, K.B., 2023. Fruit sizing in orchard: a review from caliper to machine vision with deep learning. Sensors 23, 3868. https://doi.org/10.3390/s23083868.
Orth, R.J., Carruthers, T.J.B., Dennison, W.C., Duarte, C.M., Fourqurean, J.W., Heck, K. L., Jr, Hughes, A.R., Kendrick, G.A., Kenworthy, W.J., Olyarnik, S., Short, F.T., Waycott, M., Williams, S.L., 2006. A global crisis for seagrass ecosystems. Bioscience 56, 987–996. https://doi.org/10.1641/0006-3568(2006)56[987:AGCFSE]2.0.CO;2.
Pereda-Briones, L., Infantes, E., Orfila, A., Tomas, F., Terrados, J., 2018. Dispersal of seagrass propagules: interaction between hydrodynamics and substratum type. Mar. Ecol. Prog. Ser. 593, 47–59. https://doi.org/10.3354/meps12518.
Pinna, F., Commisso, M., Guzzo, F., Bagella, S., Ceccherelli, G., Becca, G., Usai, M.F., Stipcich, P., 2026. Exploring the anatomical and metabolomic variabilities in the seagrass *Posidonia oceanica* (L.) Delile fruits. Mar. Biol. 173, 6. https://doi.org/10.1007/s00227-025-04758-6.
Poulos, S.E., 2023. Water masses of the Mediterranean Sea and Black Sea: an overview. Water 15, 3194. https://doi.org/10.3390/w15183194.
Povilus, R.A., Losada, J.M., Friedman, W.E., 2015. Floral biology and ovule and seed ontogeny of *Nymphaea thermarum*, a water lily at the brink of extinction with potential as a model system for basal angiosperms. Ann. Bot. 115, 211–226. https://doi.org/10.1093/aob/mcu235.
Provera, I., Martinez, M., Zenone, A., Giacalone, V.M., D'Anna, G., Badalamenti, F., Procaccini, G., 2024. Exploring priming strategies to improve stress resilience of *Posidonia oceanica* seedlings. Mar. Pollut. Bull. 200, 116057. https://doi.org/10.1016/j.marpolbul.2024.116057.
Rasheed, M.A., 2004. Recovery and succession in a multi-species tropical seagrass meadow following experimental disturbance: the role of sexual and asexual reproduction. J. Exp. Mar. Biol. Ecol. 310, 13–45. https://doi.org/10.1016/j.jembe.2004.03.022.
Remizowa, M.V., Sokoloff, D.D., Calvo, S., Tomasello, A., Rudall, P.J., 2012. Flowers and inflorescences of the seagrass Posidonia (Posidoniaceae, Alismatales). Am. J. Bot. 99, 1592–1608. https://doi.org/10.3732/ajb.1200227.
Ruiz-Montoya, L., Lowe, R.J., van Niel, K.P., Kendrick, G.A., 2012. The role of hydrodynamics on seed dispersal in seagrasses. Limnol. Oceanogr. 57, 1257–1265. https://doi.org/10.4319/lo.2012.57.5.1257.
Ruocco, M., Lacorata, G., Palatella, L., Provera, I., Zenone, A., Martinez, M., Dattolo, E., Pazzaglia, J., Giacalone, V.M., Badalamenti, F., Procaccini, G., 2025. Movement ecology of a coastal foundation seagrass species: insights from genetic data and oceanographic modelling. Divers. Distrib. 31, e13944. https://doi.org/10.1111/ddi.13944.
Sarneel, J.M., Beltman, B., Buijze, A., Groen, R., Soons, M.B., 2014. The role of wind in the dispersal of floating seeds in slow flowing or stagnant water bodies. J. Veg. Sci. 25, 262–274. https://doi.org/10.1111/jvs.12074.
Saunders, M.I., Cannard, T., Fischer, M., Sheppard, M., Twomey, A., Morris, R., Bishop, M.J., Mayer-Pinto, M., Malcolm, F., Vozzo, M., Steven, A., Swearer, S.E., Lovelock, C.E., Pomeroy, A.W.M., McLeod, I., Waltham, N.J., 2024. A roadmap to coastal and marine ecological restoration in Australia. Environ. Sci. Policy 159, 103808. https://doi.org/10.1016/j.envsci.2024.103808.
Schön, J.H., 2015. Density. In: Developments in Petroleum Science, 65. Elsevier, pp. 109–118. https://doi.org/10.1016/B978-0-08-100404-3.00004-4.
Sutera, A., Bonaviri, C., Spinelli, P., Carimi, F., De Michele, R., 2024. Fruit encasing preserves the dispersal potential and viability of stranded *Posidonia oceanica* seeds. Sci. Rep. 14, 6218. https://doi.org/10.1038/s41598-024-56536-x.
United Nations Environment Programme (2020). Out of the blue: The value of seagrasses to the environment and to people. UNEP, Nairobi.
Unsworth, R.K.F., Nordlund, L.M., Cullen-Unsworth, L.C., 2019. Seagrass meadows support global fisheries production. Conserv. Lett. 12, e12566. https://doi.org/10.1111/conl.12566.
van der Stocken, T., De Ryck, D.J.R., Balke, T., Bouma, T.J., Dahdouh-Guebas, F., Koedam, N., 2013. The role of wind in hydrochorous mangrove propagule dispersal. Biogeosciences 10, 3635–3647. https://doi.org/10.5194/bg-10-3635-2013.
van der Stocken, T., Vanschoenwinkel, B., De Ryck, D.J.R., Bouma, T.J., Dahdouh-Guebas, F., Koedam, N., 2015. Interaction between water and wind as a driver of passive dispersal in mangroves. PLoS. One 10, e0121593. https://doi.org/10.1371/journal.pone.0121593.
van der Stocken, T., Carroll, D., Menemenlis, D., Simard, M., Koedam, N., 2019. A general framework for propagule dispersal in mangroves. Biol. Rev. 94, 1547–1575. https://doi.org/10.1111/brv.12514.
Waycott, M., Duarte, C.M., Carruthers, T.J.B., Orth, R.J., Dennison, W.C., Olyarnik, S., Calladine, A., Fourqurean, J.W., Heck, K.L., Jr, Hughes, A.R., Kendrick, G.A., Kenworthy, W.J., Short, F.T., Williams, S.L., 2009. Accelerating loss of seagrasses across the globe threatens coastal ecosystems. Proc. Natl. Acad. Sci. USA 106, 12377–12381. https://doi.org/10.1073/pnas.0905620106.
Xu, D., Cui, J., Bansal, R., Hao, X., Liu, J., Chen, W., Peterson, B.S., 2009. The ellipsoidal area ratio: an alternative anisotropy index for diffusion tensor imaging. Magn. Reson. Imaging 27, 311–323. https://doi.org/10.1016/j.mri.2008.07.018.
Zenone, A., Badalamenti, F., Alagna, A., Gorb, S.M., Infantes, E., 2022. Assessing tolerance to the hydrodynamic exposure of *Posidonia oceanica* seedlings anchored to rocky substrates. Front. Mar. Sci. 8, 788448. https://doi.org/10.3389/fmars.2021.788448.